J. Fluid Mech. (2010), *vol.* 650, *pp.* 119–129.
doi:10.1017/S0022112010000297

Formation of turbulent patterns near the onset of transition in plane Couette flow

Y. DUGUET[1,2]†, P. SCHLATTER[1] AND D. S. HENNINGSON[1]

[1]Linné Flow Centre, KTH Mechanics, SE-10044 Stockholm, Sweden

[2]LIMSI-CNRS, UPR 3251, 91403 Orsay, France

(Received 4 September 2009; revised 14 January 2010; accepted 14 January 2010)

The formation of turbulent patterns in plane Couette flow is investigated near the onset of transition, using numerical simulation in a very large domain of size $800\,h \times 2\,h \times 356\,h$. Based on a maximum observation time of 20 000 inertial units, the threshold for the appearance of sustained turbulent motion is $Re_c = 324 \pm 1$. For $Re_c < Re \leqslant 380$, turbulent-banded patterns form, irrespective of whether the initial perturbation is a noise or localized disturbance. Measurements of the turbulent fraction versus Re show evidence for a discontinuous phase transition scenario where turbulent spots play the role of the nuclei. Using a smaller computational box, the angle selection of the turbulent bands in the early stages of their development is shown to be related to the amplitude of the initial perturbation.

1. Problem description

Plane Couette flow (pCf), the flow between two parallel walls moving in opposite directions, is the simplest canonical example of the effect of shear on a viscous fluid. The only non-dimensional parameter ruling the flow is the Reynolds number, here defined as $Re = Uh/\nu$, where $\pm U$ is the velocity of the two walls, h is the half-gap between them and ν is the kinematic viscosity of the fluid. We are interested in the way sustained turbulence appears in this system around the onset of transition. Now pCf does not belong to the class of fluid systems undergoing transition through successive losses of stability of the base flow (as, for example, Rayleigh–Bénard convection). The laminar base flow is linearly stable for all values of Re (Romanov 1973), hence transition is subcritical and is necessarily due to a finite-amplitude instability of the base flow (see for instance Schmid & Henningson 2001). Experimental investigation in a large set-up (Bottin & Chaté 1998) has shown the existence of a critical value $Re = Re_c = 323 \pm 2$, below which turbulence can be sustained over large observation times without relaminarization. The likelihood of a given disturbance to suddenly decay depends on the exact shape of the initial condition itself as well as its amplitude, hence the value of Re_c is defined only statistically. Importantly, the flow during transition shows clear signs of spatio-temporal intermittency. Experiments focusing on the ability of localized disturbances to trigger the whole flow to become turbulent yield values of Re_c from 320 to 370, corresponding to the development of a turbulent 'spot' (Daviaud, Hegseth & Berg 1992; Tillmark & Alfredsson 1992; Dauchot & Daviaud 1995; Hegseth 1996). Later experiments by the Saclay team

† Present address: LIMSI-CNRS, UPR 3251, Université Paris-Sud, 91403 Orsay, France. Email address for correspondence: duguet@mech.kth.se

in an even larger domain lead to a more accurate regime diagram parametrized by Re (Prigent *et al.* 2002; Prigent 2003). By adiabatically reducing Re from a fully turbulent field they identified a stable turbulent regime with an alternance of turbulent and laminar regions, forming for $325 < Re < 413$ a regular or sometimes fragmented pattern, oblique with respect to the direction of motion of the walls. This regime seems analogous to the 'spiral turbulence' observed experimentally in the flow between two concentric counter-rotating cylinders (Coles 1965; Van Atta 1966; Colovas & Andereck 1997; Prigent *et al.* 2002). In order to study the formation of these large-scale patterns, we chose to perform direct numerical simulations (DNS) of pCf in a periodic domain which is unusually large in the two in-plane directions. Let L_z be the spanwise extent of the numerical domain. In terms of order of magnitude, $L_z \sim O(5\,h)$ captures the local dynamics of a pair of streaks and the self-sustaining process responsible for the maintenance of a turbulent flow (Hamilton, Kim & Waleffe 1995). $L_z \sim O(20\,h)$ allows one to simulate the collective dynamics of neighbouring streaks (Komminaho, Lundbladh & Johansson 1991). For $L_z \sim O(40\text{–}100\,h)$, localized turbulence and laminar-turbulent interfaces appear, capturing the initial stage of the growth of turbulent spots (Lundbladh & Johansson 1991) and the structure of a single turbulent band (Barkley & Tuckerman 2005). The collective behaviour of spots, as well as the pattern formation resulting from their interaction, requires the whole domain to be at least one order of magnitude larger. In the framework of spatio-temporal intermittency, Pomeau (1986) used an analogy with thermodynamic phase transition and suggested that the formation of turbulent patterns corresponds to the competition between a laminar and a turbulent phase. Extending the size of the domain to study the phase transition thus corresponds to an extra step towards the 'thermodynamic limit' (Manneville 2009).

We present here numerical experiments in a periodic domain of size $(L_x, L_z) = (800\,h, 356\,h)$. For the sake of comparison, the set-up used by Prigent (2003) and Bottin *et al.* (1998a), respectively, have size $(770\,h, 340\,h)$ and $(380\,h, 70\,h)$. We use a spectral code to advance the incompressible Navier–Stokes equations in time, where the velocity field is expanded in a basis of Fourier modes (in the x- and z-directions) and Chebyshev polynomials (in the wall-normal direction y) (Chevalier *et al.* 2007). The boundary conditions are periodicity in x and z and no-slip at the walls ($y = \pm h$). The numerical resolution is 2048 spectral modes in x, 33 in y and 1024 in z. Since the wall-parallel directions are de-aliased using the 3/2 rule, the actual number of collocation points in physical space is increased by a factor of 1.5. The adequacy of the present resolution was checked by considering a smaller domain and comparing results obtained with two additional resolutions using half and twice the number of grid points in each direction. The results show that the present resolution accurately captures the localization of the turbulent patterns and statistical measures such as turbulent energies. However, we also note that in order to study other aspects of the flow, e.g. steady states or periodic solutions, a higher resolution might be necessary. Each simulation was run on up to 256 parallel processors using MPI techniques and corresponds to roughly one year of CPU time (on a single processor) each.

2. Description of the transition process

We first investigate transition to turbulence when the initial velocity field is spatially non-localized uncorrelated noise, independent of Re. The large size of the domain allows, to a first approximation, to replace costly ensemble averages by spatial averages. Because of the subcritical nature of the process, the amplitude of the initial

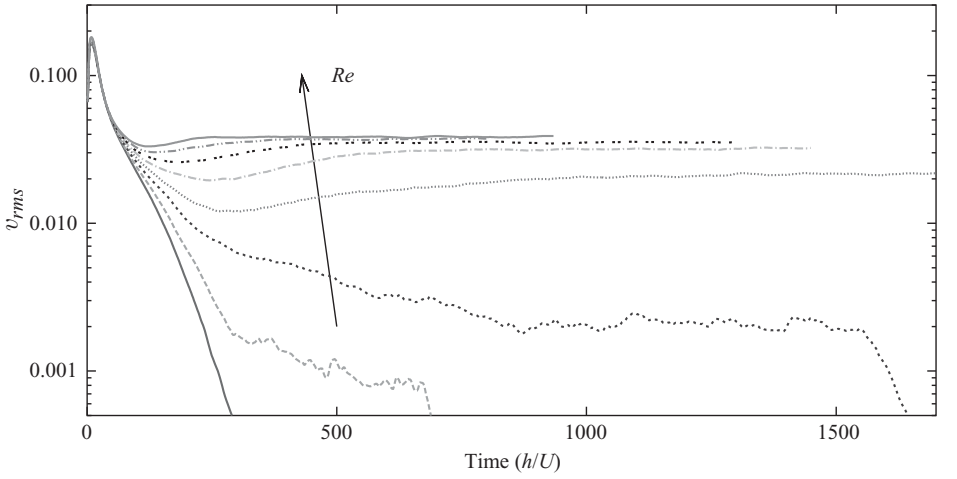

FIGURE 1. Wall normal velocity v_{rms} integrated over the whole domain, as a function of time for values of Re in the range 300–370, with increments of 10. All simulations up to $Re = 323$ eventually relaminarize, which corresponds to vanishing v_{rms} for large time $t < t_{max}$.

perturbation is chosen sufficiently large to trigger transition to turbulence as soon as $Re > Re_c$. Simulations were carried out for values of Re between $Re = 300$ and 420 with increments of 10 (refined around Re_c). The nature of the asymptotic regime can be deduced directly from the time evolution of space-averaged v_{rms} fluctuations, where v is the wall-normal velocity in the flow (see figure 1). The maximum observation time is $t_{max} = 20\,000(h/U)$. For $Re \leqslant 323$, the flow eventually returns to the laminar state ($v_{rms} = 0$). For $Re \geqslant 330$, the v_{rms} fluctuations reach a plateau, indicating sustained turbulent motion. The threshold for transition associated to this value of t_{max} is found to be $Re_c = 324 \pm 1$, in excellent agreement with threshold values in the largest experimental set-ups (Dauchot & Daviaud 1995; Bottin *et al.* 1998a; Prigent 2003).

We begin by describing the transient dynamics observed in the case $300 \leqslant Re \leqslant 323$. The initial noise dissipates quickly, giving rise after $30(h/U)$ to decaying streamwise streaks of spanwise wavelength $O(3\text{–}4h)$ (Bottin *et al.* 1998*b*). Localized zones of spatial disorder and higher intensity, i.e. turbulent 'spots', appear at random locations. The instantaneous nucleation of these spots results from the local competition between the viscous decay of streaks – on a time-scale of $O(Re)$ – and their instability, induced by the residual noise and leading to their breakdown. The number of spots nucleating from our initial condition increases smoothly with Re. As time evolves, these localized structures take an ellipse-like shape, encircling an active zone of streaks of larger amplitude. For $Re \leqslant 323$, each of those turbulent spots has a finite lifetime, so that the whole flow eventually returns to a global laminar state once each spot has decayed. In our numerical experiments, the mean lifetime of transient spots clearly increases with Re, consistently with statistical analysis (Bottin & Chaté 1998). For $Re = 320$ and $Re = 323$, the lifetime of some of the spots is long enough to display a complex dynamics: spots sometimes split in two, decay partially or drift slowly in unpredictable directions.

The early stages of the numerical experiments for $Re \geqslant 325$ are identical to the $Re = 320$ case up to $t = 400(h/U)$. However, while some of the spots at $Re = 325$ are still observed to decay, the strongest survive and unambiguously grow in size. A striking feature of the spot expansion is their oblique growth. For $330 \leqslant Re \leqslant 350$, all

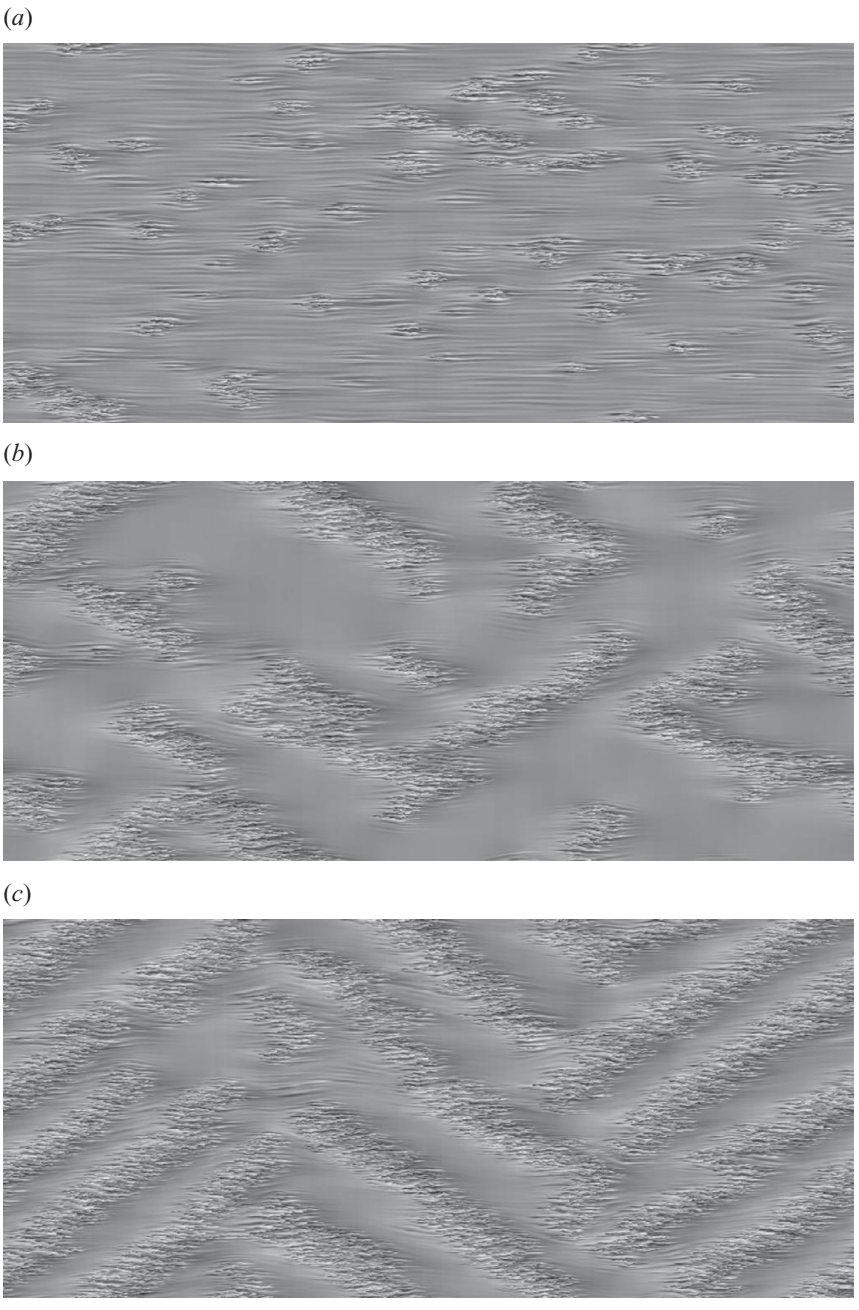

FIGURE 2. Development of a turbulent pattern at $Re = 330$ starting from a noisy initial condition. Streamwise velocity field in the mid-plane $y = 0$ at time $t = 200, 1865$ and $20\,000$ (h/U).

the spots reaching the nucleation stage are observed to grow obliquely, following a clear sequence noise → streaks → spot nucleation → stripes (see figure 2). When two neighbouring growing spots approach each other, they merge to produce one single stripe. Both positive and negative values of β coexist, where β is the angle of a band with respect to the streamwise direction x. Turbulent bands with various angles can

coexist, thus the angle β is not uniquely defined and is distributed with a spread of $\pm 10^\circ$. However, the median value of β is seen to decrease monotonically with increasing Re, in agreement with Prigent's observations (2003). It is close to $36^\circ \pm 10^\circ$ for $Re = 325$ and it approaches smoothly the angle of the diagonal of the computation domain (24°) for $Re \lesssim 350$. From $Re = 330$ to $Re = 380$, a complex pattern, consisting of alternating laminar and turbulent bands, eventually fills up the whole numerical domain. Note that when Re approaches Re_c from above (e.g. $Re = 325$), the time needed for stripes to invade the whole domain diverges because the propagation velocity of the fronts vanishes. For $Re \geqslant 330$, statistically steady patterns are usually reached after a time of $O(1000\, h/U)$. They invariably consist of fragmented turbulent stripes. However, the pattern still evolves on a slower time-scale, due to the slow propagation of topological defects, even if the level of the v_{rms} fluctuations stays statistically steady. Depending on the value of Re, various spatial arrangements of the stripes are observed, despite a similar initial condition. Perfectly aligned patterns, where all stripes are parallel to each other, such as those observed in pCf and Taylor–Couette experiments (Prigent 2003) and modelled by Barkley & Tuckerman (2005), are not observed here when starting from random noise. For a same value of Re, various wavelengths between $50\,h$ and $100\,h$ can coexist inside an equilibrium pattern (see figure 2*c*). Visualization of the cross-sectional flow (not shown) shows that the pattern is essentially two-dimensional, with a shear-induced distortion in the xy-plane. Animations of the cases $Re = 320$ and $Re = 350$ are available online.

Above $Re = 360$, the spatial density of nucleating spots becomes so large that individual spots can hardly be distinguished one from another, and the whole domain becomes quickly entirely turbulent. For Re up to 420, laminar regions can still be observed by eye in the xz-plane. These laminar zones emerge spontaneously and transiently out of the turbulent flow (whereas for $Re \leqslant 350$, the turbulent fluctuations progressively invade the laminar domain). Turbulent stripes still emerge eventually, but are less and less well-defined as Re is increased, making the Re-evolution of the angle β difficult to track. As Re is increased up to 420, laminar sub-domains are observed to shrink in size and lose their oblique orientation. At $Re = 400$ and 420, individual holes – of the width of one to two streaks – survive only transiently. This is to conform to the suggestion of an unsteady contamination process of local laminar domains by the turbulent surroundings, discussed in various models for shear flows (Manneville 2005; Lagha & Manneville 2007; Manneville 2009). The typical width of a pair of streaks, of $O(3\,h)$, is the smallest spatial scale above which it is still possible to distinguish between turbulent and laminar dynamics. This makes the identification of an upper threshold for uniform turbulence ambiguous.

Post-processing of the velocity field was done in order to accurately measure the turbulent fraction F_T as a function of Re when a steady regime is reached. F_T is defined as the area filled with turbulent motion, normalized by the area $L_x L_z$ of the whole domain. We base the determination of F_T on the fraction of the domain having a turbulent production above a certain threshold. Because laminar-turbulent patterns are only weakly dependent on the direction y, the turbulent production is evaluated in the mid-plane $y = 0$ only. The value of F_T at equilibrium is found after repeated applications of a median filter. It is shown in figure 3. For the sake of comparison, the turbulent fraction corresponding to all the transient spots near their nucleation time is also indicated in figure 3. Only the values of $Re \geqslant 330$, for which F_T has reached a statistically steady plateau at $t = t_{max}$, are shown in figure 3. For instance, $F_T(Re = 325)$ is believed not to have converged to a statistically steady value yet at $t = t_{max}$ (we have $F_T(t = t_{max}) = 0.214$), hence it is not shown in figure 3. On the contrary, the

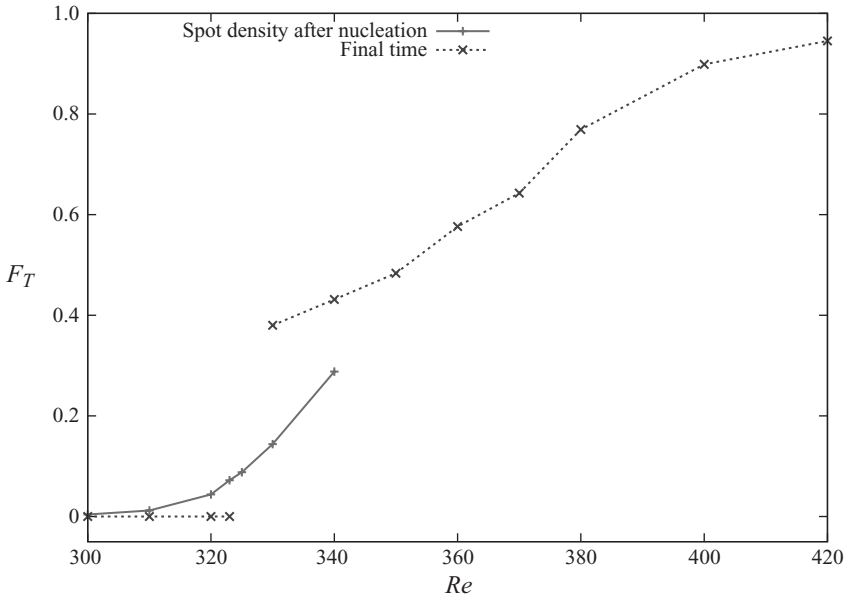

FIGURE 3. Turbulent fraction F_T as a function of Re. The dotted line corresponds to the value at equilibrium. The solid line corresponds to the turbulent fraction of the spots at nucleation time.

time-dependent quantity $F_T(Re = 330)$ varies by less than 2.5 % around its mean value 0.38 over a time interval of 10^4 (h/U), which suggests that $F_T(Re = 330) = 0.38$ is a converged value. There is, hence, a steep rise of F_T between $Re = 323$ and $Re = 325$, associated to the formation of sustained turbulent structures of finite spatial extent. F_T evolves smoothly towards unity as Re approaches 420, and there is no sharp threshold for the transition from a banded to a 'uniform' regime. Figure 3 can be interpreted as a bifurcation diagram for turbulent pCf. It is similar to that by Bottin *et al.* (1998b), however the existence of banded patterns is here clearly identified, and the singularity near Re_c is a sharp one. The analogy between this transition mechanism and thermodynamic phase transition is straightforward if F_T is interpreted as an order parameter and Re is associated to the temperature of the system. The results above clearly support a discontinuous (first-order) phase transition near $Re_c \sim 324$ and a continuous (second-order) transition to uniform turbulence around $Re = 400$. Even if discontinuity of F_T near Re_c occurs in principle only at the thermodynamic limit, the rounding-off is expected to scale like L^{-2} and thus to be weaker for larger and larger domains (Imry 1980). This singularity is linked to the nucleation of growing turbulent spots and corresponds to the minimal width of the resulting turbulent stripes. The slow increase in F_T with Re illustrates a weakening of the anisotropic mechanisms limiting the propagation of the laminar/turbulent interfaces. The analogy with first-order phase transition also implies a finite correlation length (Binder 1987) between nucleating spots, which we can estimate to be of the order of the wavelength of the turbulent stripes.

3. Localised disturbances

Given the role of growing turbulent spots in the formation of banded patterns and the finite correlation distance mentioned above, we investigate now the dynamics of a single localized disturbance free from any mutual interaction. We focus here on the

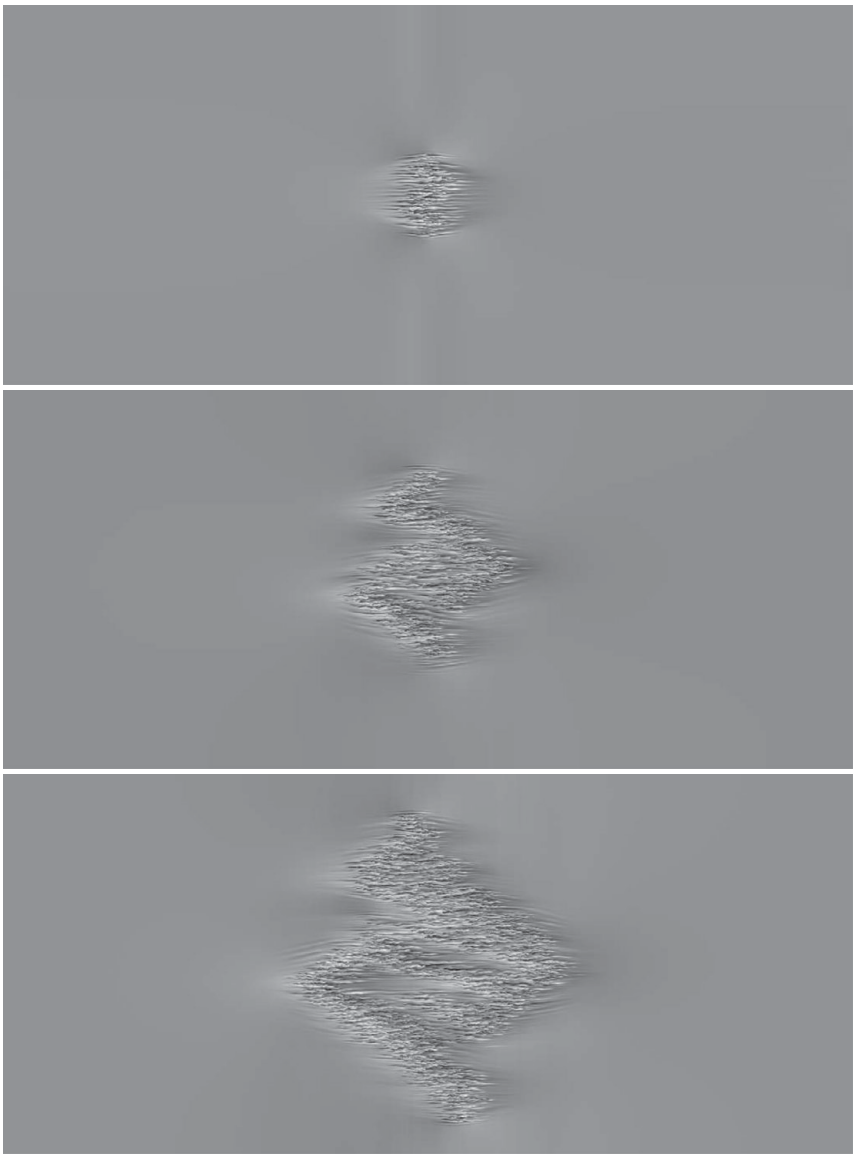

FIGURE 4. Development of a turbulent spot at $Re = 350$, starting from a localized disturbance. Streamwise velocity field in the mid-plane $y = 0$ at time $t = 201, 1043$ and 2102 (h/U). Supplementary movie available at journals.cambridge.org/flm

values of Re for which turbulent bands form, and we refer to the description by Lundbladh & Johansson (1991) Tillmark & Alfredsson (1992) for larger values of Re. The numerical domain is the same as in § 2 and we trigger spots using a localized initial condition. The very large size of the domain ensures that the growing spot (at least in the early stage of its spatial development) is not affected by the 'neighbours' resulting from the periodic boundary conditions. The initial condition is similar to that used by Lundbladh & Johansson (1991), but without the imposed spanwise symmetry; the flow outside a circle of radius $10\,h$ is initially strictly laminar. The growth of a spot at $Re = 350$ is visualized in figure 4, using the streamwise velocity in the midplane $y = 0$, and the corresponding Supplementary movie is available at journals.cambridge.org/flm. The

flow evolves quickly into a localized structure with a rhomb/ellipse shape, dominated by streaks. It is very similar to the structure observed numerically and experimentally by Lundbladh & Johansson (1991) and experimentally by Tillmark & Alfredsson (1992) at $Re = 375$ and above. The fronts of the spot initially travel with a constant velocity, resulting in a spatial expansion of the turbulent phase. The departure from previous spot studies starts around $t \sim 170\,h/U$. The spot starts to distort and takes an S-shape, symmetric around the origin (despite the lack of initial symmetry). The structure later continues to grow by increasing in length, but keeping a constant width. This dynamics evokes the formation of standing-wave labyrinths through a front instability, occurring in other diffusive systems (Yochelis *et al.* 2002). At $t > 500\,h/U$, the turbulent pattern is clearly made of several adjacent bands with various orientations. These turbulent bands, analogous to those in figure 2, have an angle β between $\pm 27^\circ$ and $\pm 56^\circ$. Spanwise ($\beta = 90^\circ$) or streamwise ($\beta = 0^\circ$) spreading sometimes occurs but inevitably leads to a splitting of the new germ, followed by its instantaneous relaminarization. This dynamics is consistent with the observation that horizontal or vertical turbulent bands cannot be sustained in pCf (cf. figure 29 in Barkley & Tuckerman 2007), and justifies qualitatively the oblique nature of the resulting fronts. This calculation demonstrates that the formation of banded patterns does not necessary result from the merging of spots, but can occur also from a single nucleation event.

4. Angle selection

In order to study which angle is preferably selected by growing spots, we adopt a numerical trick used by Barkley & Tuckerman (2005), where the angle of the stripe is constrained artificially by the periodicity of the boundary conditions. A square domain of size $(L_x, L_z) = (80, 80)$ is considered in this section, which is discretized using 128 spectral modes in each direction. This resolution is lower than the one employed in the previous sections, a choice made necessary by the many costly computations. A resolution check shows that the coarse discretization causes a shift in Reynolds number, i.e. spots generate turbulent bands, yet at a slightly lower Re than in the fully resolved case and in experiments. Note, however, that the conclusions will be unaffected by this shift in Re. The base flow is here tilted by an angle θ with respect to the x-direction in the xz-plane. For instance, $\theta = 0^\circ$ corresponds to x coinciding with the physical streamwise direction. Suppose that a turbulent band forms in this periodic domain, with an angle β with respect to the flow direction. Because of the periodicity in the x-and z-directions, the direction of the band with respect to the baseflow has no choice but to align with the x-direction, the z-direction or the xz-diagonal. This leads to $\theta + \beta = 0$, 45° or 90°, thus the angle β must be θ, $90^\circ - \theta$ or $45^\circ - \theta$. Our aim is to study how the critical amplitude of a given initial disturbance varies with θ (and hence with β). The initial condition is of the same kind as in § 3. It is tilted by θ in order to keep the same orientation with respect to the base flow as θ is varied. The constrained geometry, as well as the coarser spectral representation (compared to §§ 2 and 3), suggests to view this system only as an intermediate-order model for the formation of banded patterns. The critical amplitude A_c associated to the initial perturbation is determined by excess using a standard bisection algorithm, within an accuracy of five digits. By construction, when a perturbation of amplitude A_c evolves in time, it approaches the edge state of the system. This edge state appears to be localized in both x-and z-directions (Duguet, Schlatter & Henningson 2009). For $330 \leqslant Re \leqslant 360$ the perturbation later evolves into a turbulent band (see figure 5). Note that for $\theta = 0^\circ$ or 10°, the evolution of the fronts is strongly intermittent; no

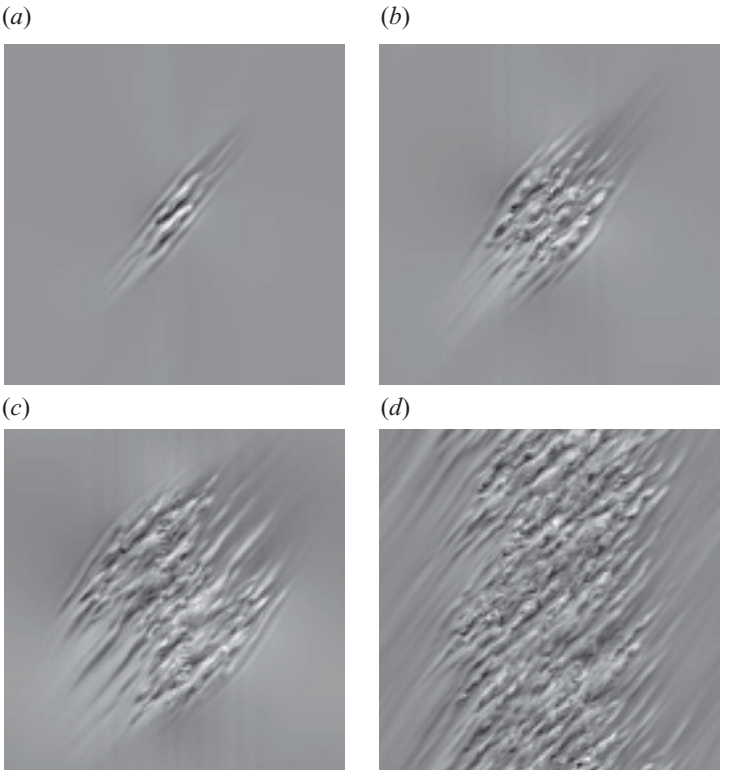

FIGURE 5. Snapshots during the formation of a turbulent band starting from the edge state, for $Re = 330$. The periodic domain has size $(L_x, L_z) = (80, 80)$ and the base flow is oriented with an angle $\theta = 50^\circ$ with respect to the x-direction. The resulting turbulent band has an orientation of $\beta = 40^\circ$ with respect to the base flow. (a–d) $t = 14,\ 37,\ 67,\ 251$ (h/U).

turbulent band can sustain, hence no angle β can be defined. For Re between 360 and 380, no turbulent band is observed, despite the presence of laminar sub-domains. The central result of this section is in figure 6. It shows the dependence of the threshold amplitude A_c on the observed angle β, in case an unambiguous turbulent band has formed. There is a clear minimum at $\beta \sim 40^\circ$, apparently independent of Re for this computational box. Assuming that the shift in Reynolds number is the main consequence of the lower resolution, these results suggest that patterns with an angle $\beta \sim 40^\circ$ need less initial energy to be sustained. Increasing the amplitude of a given localized perturbation further away from the threshold leads to a broader and continuous range of angles selected by the system. Values of $\beta \leqslant 20^\circ$ or $\beta \geqslant 70^\circ$ have not been observed, in good agreement with Barkley & Tuckerman (2007) and with the observations in §§ 2 and 3. Extending this conclusion to larger domains suggests that one preferred angle, close to 40°, is more likely to emerge in the early stages of the development of turbulent bands.

5. Conclusion

In summary, we present a bifurcation diagram of turbulent pCf, based on DNS of the incompressible Navier–Stokes equations. The use of a large computational domain is crucial for the determination of transition thresholds, because it allows to

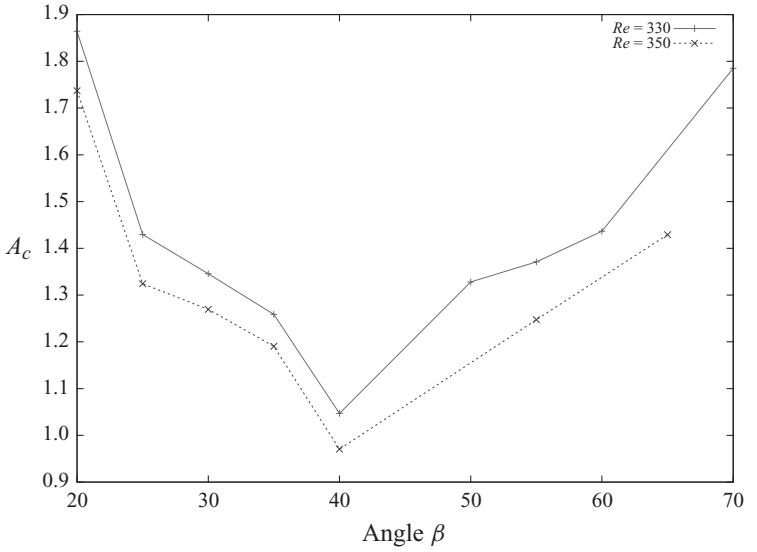

FIGURE 6. Normalized threshold amplitude A_c as a function of the angle β of the turbulent band, measured by observation with respect to the base flow direction. $Re = 330$ and $Re = 350$.

reproduce spatio-temporal intermittency structures such as transient spots, turbulent bands and laminar holes. The threshold in Re is found to be $Re_c = 324 \pm 1$, in very good agreement with available experimental data. This work points out that fragmented oblique patterns always emerge for $Re_c \leqslant Re \leqslant 380$ without hysteresis, either from the interaction of growing neighbouring spots or from the self-distortion of a single localized disturbance. The analogy with first-order thermodynamic phase transition is confirmed by the crucial role of turbulent spots as nuclei of the turbulent phase. The use of a smaller periodic domain shows that the pattern selection is intrinsically subcritical. Close to the amplitude threshold, a specific angle is selected by the system in the early stage of the growth of a turbulent band, whereas above that threshold, the range of possible angles lies between 20° and 70°.

Y. D. thanks P. Manneville for stimulating discussions. Computer time provided by SNIC (Swedish National Infrastructure for Computing) is gratefully acknowledged.

Supplementary movies are available at journals.cambridge.org/flm.

REFERENCES

BARKLEY, D. & TUCKERMAN, L. S. 2005 Computational study of turbulent-laminar patterns in Couette flow. *Phys. Rev. Lett.* **94**, 014502.

BARKLEY, D. & TUCKERMAN, L. S. 2007 Mean flow of turbulent laminar patterns in plane Couette flow. *J. Fluid Mech.* **576**, 109–137.

BINDER, K. 1987 Theory of first-order phase transitions. *Rep. Prog. Phys.* **50**, 783–859.

BOTTIN, S. & CHATÉ, H. 1998 Statistical analysis of the transition to turbulence in plane Couette flow. *Eur. Phys. J.* B **6**, 143–155.

BOTTIN, S., DAVIAUD, F., MANNEVILLE, P. & DAUCHOT, O. 1998*a* Discontinuous transition to spatiotemporal intermittency in plane Couette flow. *Europhys. Lett.* **43**, 171–176.

BOTTIN, S., DAUCHOT, O., DAVIAUD, F. & MANNEVILLE, P. 1998*b* Experimental evidence of streamwise vortices as finite amplitude solutions in transitional plane Couette flow. *Phys. Fluids* **10**, 2597–2607.

Chevalier, M., Schlatter, P., Lundbladh, A. & Henningson, D. S. 2007 A pseudo-spectral solver for incompressible boundary layer flows. *Tech. rep.* TRITA-MEK 2007:07. KTH Mechanics, Stockholm, Sweden.

Coles, D. 1965 Transition in circular Couette flow. *J. Fluid Mech.* **21**, 385–425.

Colovas, P. W. & Andereck, C. D. 1997 Turbulent bursting and spatiotemporal intermittency in the counter-rotating Taylor–Couette system. *Phys. Rev.* E **55**, 2736.

Dauchot, O. & Daviaud, F. 1995 Finite amplitude perturbation and spots growth mechanism in plane Couette flow. *Phys. Fluids* **7**, 335–343.

Daviaud, F., Hegseth, J. J. & Berg, P. 1992 Subcritical transition to turbulence in plane Couette flow. *Phys. Rev. Lett.* **69**, 2511–2514.

Duguet, Y., Schlatter, P. & Henningson, D. S. 2009 Localized edge states in plane Couette flow. *Phys. Fluids* **21**, 111701.

Hamilton, J. M., Kim, J. & Waleffe, F. 1995 Regeneration mechanisms of near-wall turbulence structures. *J. Fluid Mech* **287**, 317–348.

Hegseth, J. J. 1996 Turbulent spots in plane Couette flow. *Phys. Rev.* E **5**, 4915.

Imry, Y. 1980 Finite-size rounding of a first-order phase transition. *Phys. Rev.* B **5**, 2042–2043.

Komminaho, J., Lundbladh, A. & Johansson, A. V. 1996 Very large structures in plane turbulent Couette flow. *J. Fluid Mech.* **320**, 259.

Lagha, M. & Manneville, P. 2007 Modeling transitional plane Couette flow. *Eur. Phys. J.* B **58**, 433–447.

Lundbladh, A. & Johansson, A. V. 1991 Direct simulation of turbulent spots in plane Couette flow. *J. Fluid Mech.* **229**, 499–516.

Manneville, P. 2005 Modeling the direct transition to turbulence. In *Laminar-Turbulent Transition and Finite Amplitude Solutions* (ed. T. Mullin & R. R. Kerswell), Springer.

Manneville, P. 2009 Spatiotemporal perspective on the decay of turbulence *Phys. Rev.* E **79**, 025301.

Pomeau, Y. 1986 Front motion, metastability and subcritical bifurcations in hydrodynamics. *Physica* D **23**, 3–11.

Prigent, A. 2003 La spirale turbulente: motif de grande longueur d'onde dans les écoulements cisaillés turbulents. PhD thesis, Université Paris XI, Paris.

Prigent, A., Grégoire, G., Chaté, H., Dauchot, O. & Van Saarlos, W. 2002 Large-scale finite-wavelength modulation within turbulent shear flows. *Phys. Rev. Lett.* **89**, 014501.

Romanov, V. A. 1973 Stability of plane-parallel Couette flow. *Funct. Anal. Appl.* **7**, 137–146.

Schmid, P. J. & Henningson, D. S. 2001 *Stability and Transition in Shear Flows*. Springer.

Tillmark, N. & Alfredsson, P. H. 1992 Experiments on transition in plane Couette flow. *J. Fluid Mech.* **235**, 89–102.

Van Atta, C. W. 1966 Exploratory measurements in spiral turbulence. *J. Fluid Mech.* **25**, 495–512.

Yochelis, A., Hagberg, A., Meron, E., Lin, A. L. & Swinney, H. L. 2002 Development of standing-wave labyrinthine patterns. *SIADS* **2**, 236–247.